Chemical Science

Accepted Manuscript

This article can be cited before page numbers have been issued, to do this please use: S. Alonso-de Castro, E. Ruggiero, A. Ruiz de Angulo Caballero, E. Rezabal, J. Mareque Rivas, X. Lopez, F. Lopez-Gallego and L. Salassa, *Chem. Sci.*, 2017, DOI: 10.1039/C7SC01109A.

ROYAL SOCIETY OF CHEMISTRY

rsc.li/chemical-science

View Article Online
DOI: 10.1039/C7SC01109A

Journal Name

ARTICLE

Riboflavin As Bioorthogonal Photocatalyst For The Activation Of A Pt^{IV} Prodrug

Received 00th January 20xx,
Accepted 00th January 20xx

DOI: 10.1039/x0xx00000x

www.rsc.org/

Silvia Alonso-de Castro[a], Emmanuel Ruggiero[a], Ane Ruiz-de-Angulo[a], Elixabete Rezabal[b], Juan C. Mareque-Rivas[a,c], Xabier Lopez[d], Fernando López-Gallego[a,c], Luca Salassa*[a,c,d]

Encouraging developments demonstrate that few transition metal and organometallic catalysts can operate in a bioorthogonal fashion and promote non-natural chemistry in living systems by minimizing undesired side reactions with cellular components. These catalytic processes have potential for applications in medicinal chemistry and chemical biology. Nevertheless, the stringent conditions of the cell environment severely limit the number of accessible metal catalysts and exogenous reactions. Herein, we report an unorthodox approach and a new type of bioorthogonal catalytic reaction, in which a metal complex is an unconventional substrate and an exogenous biological molecule acts as catalyst. In such reaction, riboflavin photocatalytically converts a Pt^{IV} prodrug into cisplatin within the biological environment. The catalytic activity of riboflavin induces cisplatin-like apoptosis in cancer cells with extremely low doses of light, potentially preventing systemic off-target reactions. Photocatalytic and bioorthogonal turnover of Pt^{IV} into Pt^{II} species is an attractive strategy to amplify the antineoplastic action of metal-based chemotherapeutics with spatio-temporal control.

Introduction

The combination of catalysis and bioorthogonality[1–3] promises to impact drug discovery and bioimaging by facilitating the execution of non-natural chemical reactions in living systems. Catalytic turnover can boost the efficiency of bioorthogonal chemical reactions, unveiling new strategies for prodrug activation and uncaging of molecular probes.[4–8]

In this context, transition metal and organometallic catalysis have opened new avenues for the advance of bioorthogonal catalysis in cells.[5,9–16] The laboratories of Meggers, Mascareñas, Unciti-Broceta and Bradley used organoruthenium and palladium catalysis to deprotect pro-fluorescent substrates and activate prodrugs in cancer cells or in their compartments and surroundings.[11–14,16] Rotello devised biomimetic nanoenzymes for imaging and therapy, by encapsulating ruthenium and palladium catalysts into water-soluble gold nanoparticles and controlling their catalytic activity in HeLa cells through supramolecular chemistry.[15] These pioneering studies exploited metal-based catalytic uncaging of allylcarbamate- and propargyl-protected amines as viable strategies for bioorthogonal catalysis, however new biocompatible transformations are highly needed to further advance this extremely challenging field that is still in its infancy.

Herein, we describe an original photocatalysis approach to control the reactivity of transition metal complexes in a bioorthogonal fashion. In a new type of light-driven reaction, the exogenous biological molecule riboflavin (**Rf**) functions as a bioorthogonal photocatalyst and a metal complex as unconventional substrate (Scheme 1).

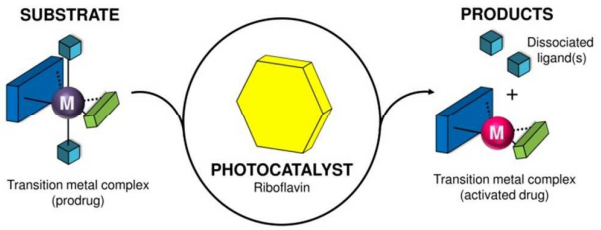

Scheme 1 Transition metal complex acting as substrate and its bioorthogonal activation by riboflavin which functions as photocatalyst.

This unusual catalyst/substrate pair relies on the photoredox properties of **Rf** to enable the selective activation of a Pt^{IV} prodrug of cisplatin with exceptionally low doses of blue light, and induce apoptotic death in PC-3 human prostate cancer cells. Metal complexes are typically regarded as catalysts which convert organic substrates in more valuable compounds, whereas catalytic transformations of metal complexes are, to date, practically unknown and represent a paradigm shift in catalysis.[17,18] Their development can expand the scope of bioorthogonal chemical reactions to inorganic substances and

[a] CIC biomaGUNE, Paseo de Miramón 182, Donostia-San Sebastián, 20014 (Spain)
[b] Farmazia Fakultatea, Kimika Fisikoa Departamentua, Euskal Herriko Unibertsitatea, UPV/EHU, Vitoria-Gasteiz, 01006 and Donostia International Physics Center (DIPC), P.K. 1072, Donostia-San Sebastián, 20080 (Spain)
[c] Ikerbasque, Basque Foundation for Science, Bilbao, 48011 (Spain)
[d] Donostia International Physics Center (DIPC), P.K. 1072, and Kimika Fakultatea, Euskal Herriko Unibertsitatea, UPV/EHU, Donostia-San Sebastián 20080 (Spain).
E-mail: lsalassa@dipc.org

† Electronic Supplementary Information (ESI) available: details on the methods employed, photocatalysis studies in solution and in biological environments, DFT calculations. See DOI: 10.1039/x0xx00000x

View Article Online
DOI: 10.1039/C7SC01109A

metal-based prodrugs, fostering the creation of new inorganic chemistry toolkits for biology and medicine.

Results and discussion

As part of our ongoing efforts to design innovative light-activation modes for anticancer platinum complexes,[19] we reasoned that **Rf** and its rich photochemistry would facilitate the photoreduction of *cis,cis,trans*-$[Pt(NH_3)_2(Cl)_2(O_2CCH_2CH_2CO_2)_2]^{2-}$ (**1**) to cisplatin by means of excitation wavelengths appropriate for use in biological systems (Scheme 2). Complex **1** is a cisplatin prodrug suitable for photochemotherapy because of its high dark stability in aqueous solutions and its negligible dark cytotoxicity in several cancer cell lines, e.g. prostate cancer PC-3 cells.[20,21]

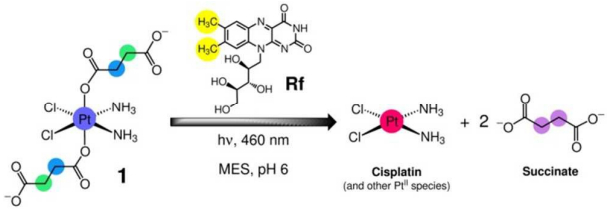

Scheme 2 Light-induced reduction of *cis,cis,trans*-$[Pt(NH_3)_2(Cl)_2(O_2CCH_2CH_2CO_2)_2]^{2-}$ (**1**) promoted by riboflavin (**Rf**) in MES buffer.

Upon UVA light excitation (385 nm) **1** undergoes photochemical activation. However, UVA light is of limited use in therapy and Pt^{IV} complexes such as **1** rarely display satisfactory absorption features at wavelengths longer than 400 nm (Fig. 1a).

Rf is vitamin B2 and the precursor of biologically important cofactors such as FMN and FAD, which are essential to humans and animals due to their redox activity.[22] The yellow-colored **Rf** absorbs in aqueous media with good extinction coefficients ($\varepsilon_{446} > 10^4$ $M^{-1}\cdot cm^{-1}$)[23] as far as ca. 500 nm (Fig. 1a), and can promote a great variety of light-induced reactions which depend on its 7,8-dimethyl-10-alkylisoalloxazine fragment.[22] **Rf** has been adopted as photocatalyst in several organic reactions, including the photooxidation of benzyl alcohols and alkyl benzenes or the [2+2] cycloaddition of styrene dienes and bis(arylenones).[24–26]

Photocatalytic activation of a Pt^{IV} prodrug by riboflavin in solution

After confirming blue light has not direct effects on **1** (Fig. S1–3†), we investigated the capability of **Rf** to photoactivate the complex upon 460-nm excitation in MES buffer. Using low excitation power density (2.5 $mW\cdot cm^{-2}$), 120 µM solutions of **1** were photolysed in the presence of **Rf** at various concentrations (12–120 µM, Fig. S4–7†). The process was monitored via ^1H NMR by the evolution of diagnostic peaks corresponding to the Pt-bound (triplets) and free (singlet) succinate ligands (Fig. 1b). Sub-stoichiometric quantities of **Rf** are capable to produce full conversion of **1** into its photoproducts under light excitation, demonstrating that **Rf** does not act as a simple photosensitizer but is indeed a photocatalyst. The efficiency of this catalytic process is remarkable since 12 µM **Rf** converts 100% of 120 µM **1** in 5 minutes (light dose 0.75 $J\cdot cm^{-2}$). A **Rf** concentration as low as 0.13 µM still photocatalyses the transformation of **1** (120 µM), however more than 2 hours are required to achieve 27% of conversion (Fig. S8†). No reaction between **1** and **Rf** occurs in the dark within 1 week (Fig. S9†). Interestingly, photoconversion of **1** takes place in pure water (pH 5) or in phosphate buffer (PB, 100 mM, pH 5.5), but never reaches completion due to poor photostability of **Rf** in these media (vide infra). Thus, MES buffer plays a key role in the catalytic process preventing **Rf** from undergoing photodecomposition reactions.

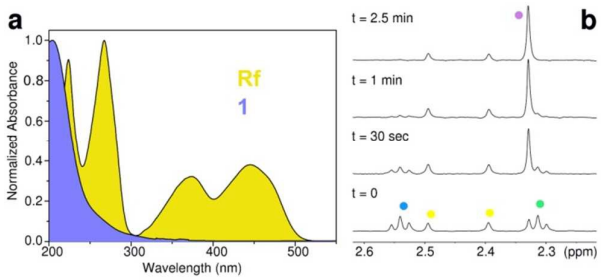

Fig. 1 (a) Absorption spectrum of riboflavin (**Rf**) and *cis,cis,trans*-$[Pt(NH_3)_2(Cl)_2(O_2CCH_2CH_2CO_2)_2]^{2-}$ (**1**) in aqueous solution. (b) **Rf**-catalysed photoreduction of **1** in MES buffer (18 mM, pH 6) monitored by ^1H NMR. Spectra were recorded for a MES/D_2O (9:1) solution of 120 µM **1** and 50 µM **Rf** upon t = 0 sec, 30 sec, 1 min and 2.5 min of 460-nm light irradiation (2.5 $mW\cdot cm^{-2}$). ^1H NMR signal labelling: ● Pt–$OCOCH_2CH_2CO_2^-$, ● Pt–$OCOCH_2\mathbf{CH_2}CO_2^-$, ● methyl groups of **Rf** isoalloxazine ring, ● free $^-O_2C\mathbf{CH_2CH_2}CO_2^-$.

In order to assess the rate law for the **Rf**-catalysed photoreduction of **1** to Pt^{II} species, we studied the reaction rate at different substrate concentrations (120 µM–1.92 mM, i.e. 2.4–38.4 mol equiv of **1** compared to **Rf**) in 18 mM MES buffer during 30 sec of irradiation at 298 K (Fig. S10†). The effect of MES on the reaction rate was evaluated in a separate set of experiments, in which MES concentration was varied in the 3–20 mM range (Fig. S11†). Results demonstrate that the rate of the reaction linearly increases with the concentration of **1** and MES, corresponding to a first-order reaction for both species. Importantly, the reaction shows a stronger dependency on the concentration of **1** than on MES, suggesting that Pt^{IV} reduction is limiting step of the reaction.

Since our experiments employ a large excess of MES and all reaction steps are irreversible, the rate constant can be described using the pseudo-first order model (ESI†). Using 50 µM **Rf**, we obtained a pseudo-first order reaction constant (k_{obs} = 10.0 ± 0.05·10^{-3} s^{-1}) that increases with the catalyst concentration (Fig. S12† and S13†) and depends on MES concentration.

A turnover frequency (TOF) value of 0.22 ± 0.06 s^{-1} was determined for the conversion of **1** (1.92 mM) by **Rf** (50 µM) under light irradiation at 298 K in 18 mM MES buffer. Under such reaction conditions, the maximum total turnover number (TTN) value is 38 after 3 minutes of light irradiation, and no decomposition of catalyst is observed by ^1H NMR. The **Rf**/**1** catalyst/substrate pair achieves approx. 700–70 times higher TOF compared to ruthenium(II) organometallic catalysts,

View Article Online
DOI: 10.1039/C7SC01109A

which catalytically convert NAD^+ in NADH or transform O-allyl carbamates into their respective amines under biologically relevant conditions and in cells.[9,8] High TOF is crucial for application in photochemotherapy since it guarantees rapid and sufficient conversion of **1** with short irradiation times and low light doses.

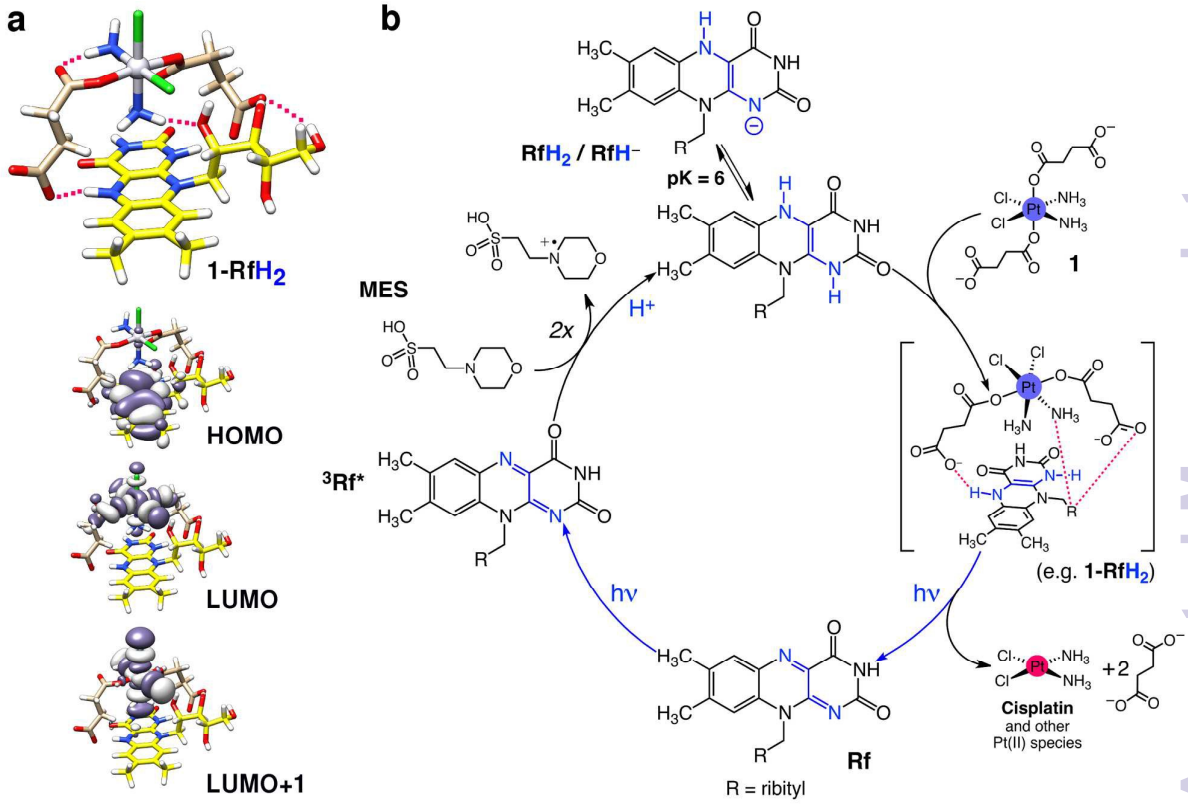

Fig. 2 Proposed mechanism for the photocatalytic activation of **1** by **Rf**. (a) Computed structure and frontier molecular orbitals (DFT:PBE0/def2-SVP) of a selected **1**-**Rf**H_2 adduct. Intermolecular H-bonds in **1**-**Rf**H_2 are highlighted with magenta lines (top). Isodensity surfaces are plotted with the isovalue of 0.02 e^-·$bohr^{-3}$. Atoms color code: Pt grey, Cl green, O red, N blue, C pale brown (**1**) or yellow (**Rf**), H white. (b) **Rf** absorbs 460-nm photons to generate the triplet

Mechanism of photocatalytic activation

Rf is extremely light sensitive and its photochemical reactivity strongly depends on the surrounding environment. Electron transfer and proton-coupled reactions or singlet-oxygen generation take place upon light excitation of **Rf**, depending on the availability of electron donors. In addition, light decomposes **Rf** into several fragments through intramolecular reactions in which the ribityl chain can be used as the electron source.[27]

Direct energy transfer from **Rf** to **1** can be ruled out since there is no overlap between the emission band of the flavin (λ_{em} = 535 nm) and the absorption spectrum of **1**.

Hence, the sensitizing and catalytic capacity of **Rf** in MES buffer reasonably relies on electron transfer processes triggered by light. In the triplet excited state (^{3}**Rf***), **Rf** is a strong oxidant (E^o = 1.77 V)[22] capable of efficiently extracting electrons from the abundant MES molecules, and generate the two-electron reduced **Rf**H_2/**Rf**H^- species (pK_a ~ 6) together with morpholino radicals[28] which eventually evolve to the oxidized N-oxide form of MES (Fig. S14†).[29]

Employing ferrioxalate actinometry,[30] we determined the photochemical quantum yield for **Rf**/**1** (50 μM / 1.0 mM, 18 mM MES) obtaining a value of 1.4 ± 0.1 (Fig. S15† and S16†). Yield values > 1 are rather common in photoredox catalysis where radical chain propagation cycles form part of the catalytic mechanism.[31]

MES buffer dramatically improves **Rf** photostability by preventing that the isoalloxazine unit reacts with the ribityl moiety or with molecular oxygen. NMR and UV-Vis show that MES substantially preserves **Rf** from decomposition for over 30 min, whereas the catalyst is fully converted to the photoproduct lumichrome in water within 1 min of light irradiation, and then to 2,3-butanedione at longer irradiation times (Fig. S17–19†).[32]

The role of the buffer was confirmed using HEPES (18 mM, pH 6), an analogue zwitterionic buffering agent (Fig. S20† and S21†), in which **Rf** and **1** behave similarly to MES in terms of photocatalytic activity.

The presence of sodium azide (singlet oxygen scavenger) in water and PB also improves the efficiency of the photocatalytic reaction of **Rf** with **1** (Fig. S22† and S23†). When added to MES buffer, sodium azide does not improve **Rf**/**1** (Fig. S24†), excluding the participation of $^1O_2$ and other oxygen radicals as major actors in the catalytic mechanism. On the other hand, O_2 partially deactivates **Rf**, since under inert Ar atmosphere the photoconversion of **1** is faster (Fig. S25†).

View Article Online
DOI: 10.1039/C7SC01109A

excited state (^{3}**Rf***) which oxidizes two MES molecules to give the reduced species **Rf**H_2/**Rf**H^-. Next, complex **1** forms stable adducts with either **Rf**H_2 (shown in Fig. 2a) or **Rf**H^- and undergoes photoreduction and elimination reactions upon absorption of more photons, liberating cytotoxic Pt^{II} species and regenerating the **Rf** catalyst.

Importantly, complex **1** (1.8 mM) does not affect the fluorescence lifetime of **Rf** in MES (Fig. S26† and S27†), indicating that the active catalyst is not likely to be a **Rf** excited-state species. Therefore, photooxidation of MES ultimately leads to the formation of reduced (ground-state) **Rf**H_2/**Rf**H^-, whose low redox potential (ca. –0.2 V)[22] cannot directly promote reduction of **1** (–0.9 V).[33]

Yet, as suggested by density functional theory (DFT) modelling (PBE0/def2-SVP) and consistently with the results obtained under Ar atmoshpere, **1** is capable to form adducts with either **Rf**H_2 (Fig. 2a) or **Rf**H^- (Fig. S28–30†) by means of H-bonding interactions between its succinate and amino ligands, and the isoalloxazine and ribityl groups of **Rf**. FMN and FAD also photocatalyze the Pt^{IV} conversion of **1**, displaying an efficiency comparable to **Rf** (Fig. S31–34†). FAD, however, is somewhat less active, possibly due to steric constrains introduced by its adenine moiety which would disfavour H-bonding between the complex and the flavin.

Computed **1**-**Rf**H_2 and **1**-**Rf**H^- adducts have HOMO localized on the **Rf** isoalloxazine rings, while LUMO and LUMO+1 are σ-antibonding orbitals of **1**. Absorption of a second photon and subsequent light-induced population of the dissociative LUMO orbitals can trigger photoreduction and ligand elimination reactions,[34] ultimately promoting the formation of cisplatin and other Pt^{II} species. Nevertheless, we cannot exclude at this stage that these strong and specific interactions could significantly lower the redox potential of **1** and cause direct reduction of the prodrug once the **Rf**-adducts are formed.[35,36] Calculated binding energy for **1**-**Rf**H_2 and **1**-**Rf**H^- adducts are in range 52–69 kcal·mol^{-1}, indicating that these transient species are strongly stabilized and may bestow unique selectivity to the **Rf**/**1** catalyst/substrate pair (vide infra).

A pH-dependency profile for the photoreaction at fixed light-irradiation time (2.5 min) shows that complete photoconversion of **1** occurs above pH 6 in MES, whereas at lower pHs the photocatalysis is less efficient (Fig S35†). The finding is in agreement with the prevalence of the **Rf**H_2/**Rf**H^- forms of reduced **Rf** at pHs higher than 6.[22]

On the basis of the described evidence, we have schematized a tentative photocatalytic mechanism for the **Rf**/**1** catalyst/substrate pair in Fig. 2b, although further investigations will be needed for its complete elucidation.

Photocatalysis in the biological environment

To test the potential of **Rf** photocatalysis as a bioorthogonal tool for photochemotherapy, we studied next the activation of **1** by **Rf** in cell culture medium and its effects in PC-3 cancer cells (in which **1** has no dark toxicity). At first, photocatalysis experiments and controls (Fig. S36† and S37†) were performed in Ham's F-12K medium supplemented with fetal bovine serum, in which biological components such as growth factors, antibodies, aminoacids, vitamins, and inorganic salts are present at concentrations ranging from μM to mM.

^{1}H NMR data showed that 3 min of blue light irradiation (light dose 1.08 J·cm^{-2}) can fully convert 1.92 mM **1** to Pt^{II} species in the presence of 50 μM **Rf** and 3 mM MES, without any significant side reaction affecting either medium components or the catalyst (Fig. S38†). Under such conditions the TOF and TTN for the **Rf** catalyst are as good as in pure MES buffer solutions, indicating that the catalytic process is bioorthogonal in cell culture medium.

The antiproliferative activity of **Rf**/**1** against PC-3 cancer cells was investigated in the dark and under 460-nm light irradiation by co-administering the catalyst/substrate pair at a molar ratio of 1:4 and using three different concentrations of complex (40, 80, 120 μM). In our cell experiments, **Rf** prevalently activates **1** in the extracellular space since we performed light irradiation after a short pre-incubation period and replaced culture medium after 6 h. Once photocatalytically generated, Pt^{II} species can be internalized by cells and exert their antiproliferative action. MES is well tolerated by cells (Fig. S39†) and was hence employed during cell viability assays as an electron donor. Under these conditions, a short light irradiation period (1 min) and an extremely low light dose (0.36 J·cm^{-2}) are sufficient for the full photoconversion of **1** by **Rf** (Fig. S40† and S41†). In the absence of MES the photoactivation of **1** still takes place, although less efficiently (Fig. S42†), likely because other biological components of the medium act as electron donors. Against PC-3 cells, the **Rf**/**1** catalyst/substrate pair displays dose- dependent light-induced toxicity comparable to cisplatin in the dark. Remarkably, 120 μM **1** and 30 μM **Rf** induce a 55 ± 5% reduction in cell biomass under light irradiation, against a 65 ± 5% caused by cisplatin at the same concentration. Control experiments indicate that **Rf**/**1** does not reduce viability of PC-3 cells when kept in the dark, neither does any of the components when irradiated individually (Fig. 3a).

The antiproliferative action of **Rf**-activated **1** is associated with the formation of cisplatin as one of the major cytotoxic photoproducts. Initial evidence was gathered from binding experiments with the RNA and DNA base model 5′-guanosin monophosphate (GMP). ^{1}H NMR shows that irradiated **Rf**/**1** solutions incubated with GMP (0–24 h) present the diagnostic peak, corresponding to the cisplatin mono GMP-Pt^{II} adduct (Fig. S43† and S44†).[37] When incubated with the pET28b as model of double stranded circular DNA (24 h, MES 1.5 mM, pH 6), light-activated **Rf**/**1** (2.5:10 μM) inhibits the polymerase chain reactions (PCR). Thirty sec of light irradiation are sufficient to stop DNA amplification and reach PCR inhibition level comparable with cisplatin (10 μM), hence confirming the capacity of this biorthogonal system to produce DNA-targeting species (Fig. S45†).[38,39]

Fluorescence microscopy of PC-3 cells treated with either irradiated **Rf**/**1** (30:120 μM) or cisplatin (120 μM) is in agreement with this scenario (Fig. 3b and Fig. S46†). In both cases, images obtained after 48 h of incubation show increased

View Article Online
DOI: 10.1039/C7SC01109A

percentage of apoptotic versus viable cells, together with changes in cell morphology that are characteristic of apoptosis, i.e. cell shrinkage and rounding. Non-treated cells and cells treated with **Rf**/**1** in the dark included as controls do not induce appreciable cell death.

Consistently, flow cytometry results confirm that PC-3 cells exposed to the **Rf**/**1** mixture and light (30:120 μM) die through apoptosis 48 hours after irradiation. Cisplatin induces comparable levels of apoptosis under the same conditions.

Double staining with Pacific Blue™ Annexin V / SYTOX® allowed differentiating between early-stage and late-stage apoptosis. Upon treatment with irradiated **Rf**/**1**, the percentage of early apoptotic cells is 16.7 ± 2.8 % against 19.9 ± 1.3 % obtained for cisplatin. **Rf**, **1** and **Rf**/**1** in the dark exhibit no significant population of cells in either stage of apoptosis after 48 h of incubation (Fig. 3c).

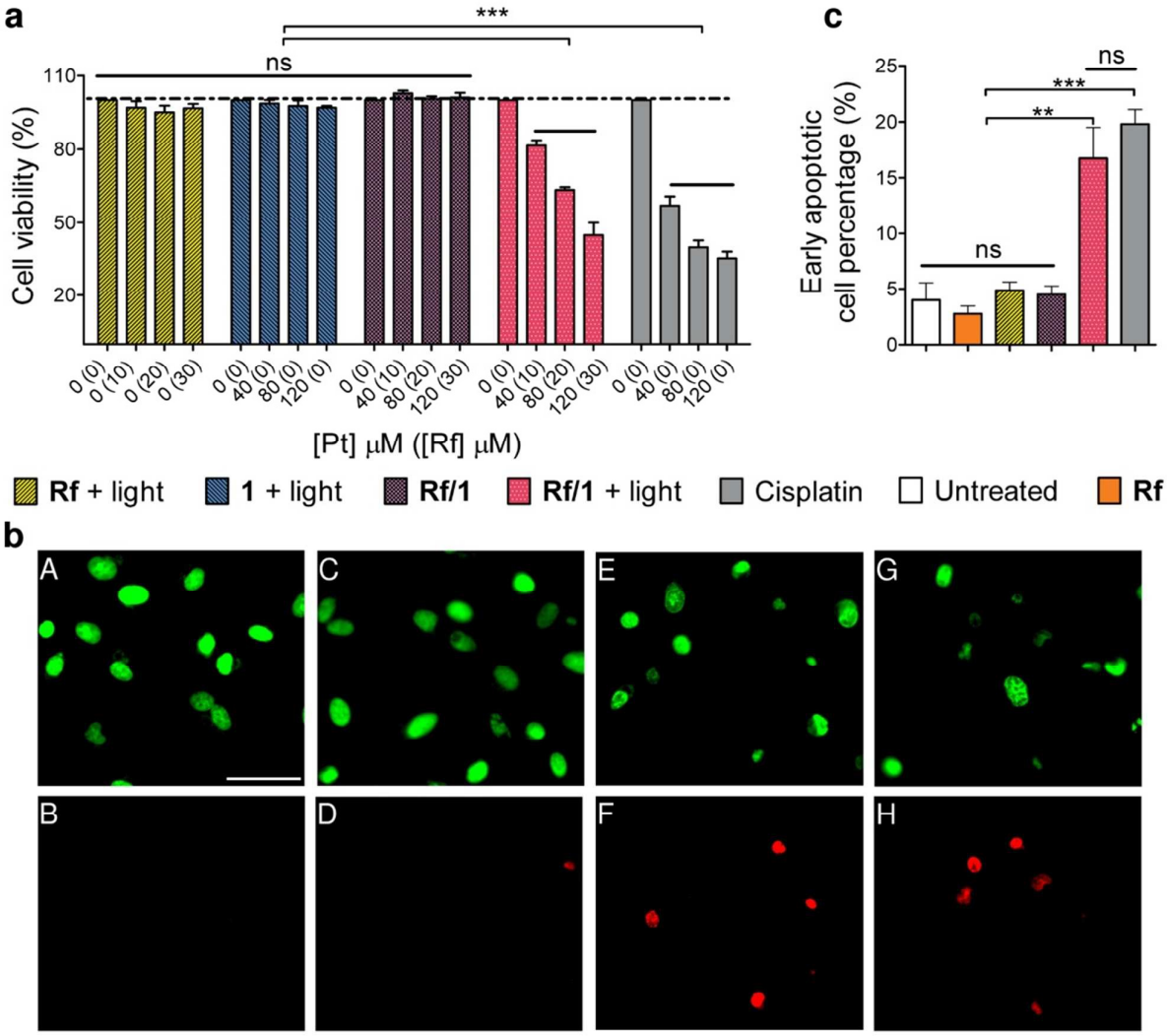

Fig. 3 Antiproliferative activity in human prostate cancer PC-3 cells. (a) Percentage cell viability of PC-3 cells following treatment with **Rf**, **1**, **Rf**/**1** and cisplatin with and/or without light activation (460 nm, 0.36 J·cm^{-2}). (b) Fluorescence microscopy images showing the effects of **Rf**/**1** on PC-3 cells upon light irradiation. (A, B) untreated PC-3 cells, (C, D) **Rf**/**1** (30:120 μM) in the dark, (E, F) **Rf**/**1** (30:120 μM) activated by 460-nm light and (G, H) cisplatin (120 μM) in the dark. Top row: cell nuclei (green); bottom row: apoptotic cells (red). (c) Quantification of early apoptotic PC-3 cells (Annexin V+ / SYTOX–) treated by **Rf** (30 μM), **Rf**/**1** (30:120 μM) and cisplatin (120 μM) with and/or without light activation. Cell viability and flow cytometry data are presented as mean ± SEM of at least three independent measurements. ***P < 0.001, **P < 0.01, ns = non-significant by two-way ANOVA followed by Bonferroni's test (a) or by one-way ANOVA followed by Tukey's test (c).

Conclusions

In summary, we have described the first photocatalytic activation of a metal-based prodrug in solution and in a biological environment. Co-administration of the **Rf**/**1** as catalyst/substrate couple enables photoconversion of **1** into

View Article Online
DOI: 10.1039/C7SC01109A

biologically active species by light irradiation at 460 nm, a wavelength that is ineffective when directly applied to the prodrug. In addition, the **Rf**/**1** prodrug activation strategy induces an anticancer activity comparable to cisplatin with light doses as low as 0.36 J·cm^{-2}, that is ca. 15–35 times lower than what is typically used for UVA and blue light activation of analogue platinum complexes.[40,41]

The photocatalytic turnover of Pt^{IV} into Pt^{II} species is an attractive prospect to amplify the antineoplastic action of metal-based prodrugs in a locoregional manner. This is particularly relevant for platinum anticancer agents, which have some of the poorest absorption properties amongst photoactivatable metal complexes, but are widely tested in preclinical work and nearly indispensable in clinical practice.

In principle, photocatalysis can help expanding the therapeutic potential of platinum prodrugs. Efficient light activation of Pt^{IV} complexes through catalysis may help localize the cytotoxic effects of Pt drugs, increase their dosing at the tumour target and reduce their systemic toxicity. **Rf** (vitamin B2) is a highly biocompatible molecule and its capacity to function in a bioorthogonal fashion may serve to enhance the selectivity of metal-based drugs by minimizing side reactions.

Experimental section

Methods. NMR, UV-Vis and fluorescence characterization of light-irradiated **Rf**/**1** and controls, PCR and microscopy data, photochemical quantum yield by actinometry, setup for cell work under light irradiation, computational methodology and instrumentation details are described in the ESI†.

Light-irradiation experiments in solution. Photocatalysis studies on **Rf**/**1** were performed under different solution conditions (buffers, cell culture medium and in presence of co-reactants). All reactions were carried out in air at 298 K and pH 6, employing an LED light source (λ_{exc} = 460 nm, 2.5 mW·cm^{-2}). Reaction kinetics, law rates of the reaction, turnover frequency (TOF) and total turnover number (TTN) were calculated by varying both reactants and catalyst concentration and quantifying via ^{1}H NMR the amount of photoconverted **1**.

Cell viability studies. The antiproliferative activity of **Rf**/**1** was determined in human prostate cancer cells PC-3 (ATCC) in the dark and under light irradiation by co-administering **Rf** and **1** at a fixed molar ratio (1:4), and using three different concentrations (**Rf**/**1**: 10/40 μM, 20/80 μM, 30/120 μM). MES was employed in all cell experiments at a final concentration of 2 mM. PC-3 cells were seeded 24 h before the experiment in 96-well plates with a density of 4000 cells per well and grown under standard conditions (Ham's F-12K medium supplemented with 10% fetal bovine serum and 1% penicillin/streptomycin at 37°C, 5% CO_2 and 90% humidity). Stock solutions of **Rf**/**1** were added and incubated with cells for 1 h, light irradiated for 1 min at 460 nm (light dose 0.36 J·cm^{-2}), and then incubated for other 6 h. Finally, cells were washed in fresh medium and grown for other 42 h. The Sulforhodamine B (SRB) colorimetric assay was used for cell density determination. As controls, **Rf** and **1** were tested under identical conditions, while parallel experiments were performed with **Rf**/**1** and cisplatin kept in the dark. A home-made LED plate was employed to irradiate cells in 96-well plates (Fig. S47†).

Fluorescence microscopy assays. PC-3 cells exposed to 30:120 μM **Rf**/**1** were viewed using a Zeiss Axio Observer wide field fluorescence microscope (Carl Zeiss). Cells were plated in an ibidi μ-Slide 0.4 (13500 PC-3 cells/channel) and allowed to adhere overnight before they were treated with **Rf**/**1** as described for cell viability experiments (2 mM MES, 6 h of treatment plus 42 h incubation). Analysis of cellular morphological alteration was performed using a cell-permeable green fluorescent dye from the "Live and Dead Cell Staining Kit" (Abcam) for cell nuclei (green channel) and SYTOX® AADvanced™ (Invitrogen™) for dead cells (red channel). Cells were stained following commercial protocols and using binding or 10 mM PBS buffer at the end of the incubation period (48 h). Images were acquired with a Plan Apochromat 20× objective and a multi-band pass Colibri filter to collect fluorescence emission signals. Control experiments in the dark (no light irradiation) were performed on untreated cells and on cells exposed to 30:120 μM **Rf**/**1** or 120 μM cisplatin.

Flow cytometry analysis. PC-3 cells were seeded in 96-well plates (2000 cells per well) and treated with **Rf**/**1** (30:120 μM) and MES (2 mM) as described above. After 48 hours of incubation, 7 wells for each sample were pooled into cytometer tubes, cells were washed with 10 mM PBS and stained using 100 μL per tube of the Pacific Blue™ Annexin V/SYTOX® AADvanced™ flow cytometry kit (Invitrogen™). Early and late apoptosis were measured using a FACS Canto II (BD Biosciences) and results analysed using the FlowJo, LCC software. The PC-3 population was electronically gated based on the forward and side scatter parameters and the non-single events leaved out based on forward area and height scatter parameters. Inside this final population, live cells were gated as negative for both dyes; early apoptotic cells were defined as Pacific Blue-Annexin V positive cells and SYTOX® negative; and late apoptotic cells were gated as double positive for both dyes. Non-labelled and singly labelled samples were included as control and as compensation samples, respectively. Experiments were repeated three times. Besides untreated cells, control experiments included cells treated with 30:120 μM **Rf**/**1** and 120 μM cisplatin in the dark (no light irradiation), and light-irradiated **Rf** and **1** alone.

Acknowledgements

This work was supported by the Spanish Ministry of Economy and Competitiveness (grant CTQ2016-80844-R and BES-2013-065642), the Department of Industry of the Basque Country (grant ETORTEK). L.S. thanks the MICINN of Spain for the Ramón y Cajal Fellowship RYC-2011-07787 and the MC CIG fellowship UCnanomat4iPACT (grant no. 321791). L.S., F.L.G. and J.M.R. thank Ikerbasque for funding. We are also grateful to the members of the European COST Actions CM1105, CM103 and CM1403 for stimulating discussions.

View Article Online
DOI: 10.1039/C7SC01109A

References

1 C. R. Bertozzi, *Acc. Chem. Res.*, 2011, **44**, 651–653.
2 E. M. Sletten and C. R. Bertozzi, *Angew. Chem. Int. Ed.*, 2009, **48**, 6974–6998.
3 D. M. Patterson, L. A. Nazarova and J. A. Prescher, *ACS Chem. Biol.*, 2014, **9**, 592–605.
4 A. Unciti-Broceta, *Nat. Chem.*, 2015, **7**, 538–539.
5 P. K. Sasmal, C. N. Streu and E. Meggers, *Chem. Commun.*, 2013, **49**, 1581–1587.
6 J. Clavadetscher, S. Hoffmann, A. Lilienkampf, L. Mackay, R. M. Yusop, S. A. Rider, J. J. Mullins and M. Bradley, *Angew. Chem. Int. Ed.*, 2016, **55**, 15662–15666.
7 S. V. Chankeshwara, E. Indrigo and M. Bradley, *Curr. Opin. Chem. Biol.*, 2014, **21**, 128–135.
8 J. T. Weiss, J. C. Dawson, C. Fraser, W. Rybski, C. Torres-Sánchez, M. Bradley, E. E. Patton, N. O. Carragher and A. Unciti-Broceta, *J. Med. Chem.*, 2014, **57**, 5395–5404.
9 J. J. Soldevila-Barreda, I. Romero-Canelón, A. Habtemariam and P. J. Sadler, *Nat. Commun.*, 2015, **6**, 6582.
10 Z. Liu, I. Romero-Canelón, B. Qamar, J. M. Hearn, A. Habtemariam, N. P. E. Barry, A. M. Pizarro, G. J. Clarkson and P. J. Sadler, *Angew. Chem. Int. Ed.*, 2014, **53**, 3941–3946.
11 T. Völker, F. Dempwolff, P. L. Graumann and E. Meggers, *Angew. Chem. Int. Ed.*, 2014, **53**, 10536–10540.
12 P. K. Sasmal, S. Carregal-Romero, W. J. Parak and E. Meggers, *Organometallics*, 2012, **31**, 5968–5970.
13 J. T. Weiss, J. C. Dawson, K. G. Macleod, W. Rybski, C. Fraser, C. Torres-Sánchez, E. E. Patton, M. Bradley, N. O. Carragher and A. Unciti-Broceta, *Nat. Commun.*, 2014, **5**, 3277.
14 R. M. Yusop, A. Unciti-Broceta, E. M. V. Johansson, R. M. Sánchez-Martín and M. Bradley, *Nat. Chem.*, 2011, **3**, 239–243.
15 G. Y. Tonga, Y. Jeong, B. Duncan, T. Mizuhara, R. Mout, R. Das, S. T. Kim, Y.-C. Yeh, B. Yan, S. Hou and V. M. Rotello, *Nat. Chem.*, 2015, **7**, 597–603.
16 M. Tomás-Gamasa, M. Martínez-Calvo, J. R. Couceiro and J. L. Mascareñas, *Nat. Commun.*, 2016, **7**, 12538.
17 L. Gong, Z. Lin, K. Harms and E. Meggers, *Angew. Chem. Int. Ed.*, 2010, **49**, 7955–7957.
18 M. Fontecave, *ChemCatChem*, 2010, **2**, 1533–1534.
19 E. Ruggiero, J. Hernández-Gil, J. C. Mareque-Rivas and L. Salassa, *Chem. Commun.*, 2015, **51**, 2091–2094.
20 I. Infante, J. M. Azpiroz, N. G. Blanco, E. Ruggiero, J. M. Ugalde, J. C. Mareque-Rivas and L. Salassa, *J. Phys. Chem. C*, 2014, **118**, 8712–8721.
21 C. R. Maldonado, N. Gómez-Blanco, M. Jauregui-Osoro, V. G. Brunton, L. Yate and J. C. Mareque-Rivas, *Chem. Commun.*, 2013, **49**, 3985–3987.
22 S. Weber and E. Schleicher, Eds., *Flavins and Flavoproteins*, Springer New York, New York, NY, 2014, vol. 1146.
23 P. F. Heelis, *Chem. Soc. Rev.*, 1982, **11**, 15–39.
24 G. de Gonzalo and M. W. Fraaije, *ChemCatChem*, 2013, **5**, 403–415.
25 C. Feldmeier, H. Bartling, K. Magerl and R. M. Gschwind, *Angew. Chem. Int. Ed.*, 2015, **54**, 1347–1351.
26 B. Mühldorf and R. Wolf, *Angew. Chem. Int. Ed.*, 2016, **55**, 427–430.
27 M. Insińska-Rak and M. Sikorski, *Chem. Eur. J.*, 2014, **20**, 15280–15291.
28 C. J. Baker, N. M. Mock, D. P. Roberts, K. L. Deahl, C. J. Hapeman, W. F. Schmidt and J. Kochansky, *Free Radic. Biol. Med.*, 2007, **43**, 1322–1327.
29 G. Zhao and N. D. Chasteen, *Anal. Biochem.*, 2006, **349**, 262–267.
30 S. L. Hopkins, B. Siewert, S. H. C. Askes, P. Veldhuizen, R. Zwier, M. Heger and S. Bonnet, *Photochem. Photobiol. Sci.*, 2016, **15**, 644–653.
31 M. A. Cismesia and T. P. Yoon, *Chem. Sci.*, 2015, **6**, 6019–6019.
32 M. A. Sheraz, S. H. Kazi, S. Ahmed, Z. Anwar and I. Ahmad, *Beilstein J. Org. Chem.*, 2014, **10**, 1999–2012.
33 P. Gramatica, E. Papa, M. Luini, E. Monti, M. B. Gariboldi, M. Ravera, E. Gabano, L. Gaviglio and D. Osella, *J. Biol. Inorg. Chem.*, 2010, **15**, 1157–1169.
34 C. Garino and L. Salassa, *Philos. Trans. R. Soc. A*, 2013, **371**, 20120134.
35 G. Thiabaud, R. McCall, G. He, J. F. Arambula, Z. H. Siddik and J. L. Sessler, *Angew. Chem. Int. Ed.*, 2016, **55**, 12626–12631.
36 A. Garaikoetxea Arguinzoniz, N. Gómez Blanco, P. Ansorena Legarra and J. C. Mareque-Rivas, *Dalton Trans*, 2015, **44**, 7135–7138.
37 F. J. Dijt, G. W. Canters, J. H. J. Den Hartog, A. T. M. Marcelis and J. Reedijk, *J. Am. Chem. Soc.*, 1984, **106**, 3644–3647.
38 C. Ducani, A. Leczkowska, N. J. Hodges and M. J. Hannon, *Angew. Chem. Int. Ed.*, 2010, **49**, 8942–8945.
39 A. Terenzi, C. Ducani, L. Male, G. Barone and M. J. Hannon, *Dalton Trans*, 2013, **42**, 11220–11226.
40 J. Kasparkova, H. Kostrhunova, O. Novakova, R. Křikavová, J. Vančo, Z. Trávníček and V. Brabec, *Angew. Chem. Int. Ed.*, 2015, **54**, 14478–14482.
41 Y. Zhao, J. A. Woods, N. J. Farrer, K. S. Robinson, J. Pracharova, J. Kasparkova, O. Novakova, H. Li, L. Salassa, A. M. Pizarro, G. J. Clarkson, L. Song, V. Brabec and P. J. Sadler, *Chem. – Eur. J.*, 2013, **19**, 9578–9591.

View Article Online
DOI: 10.1039/C7SC01109A

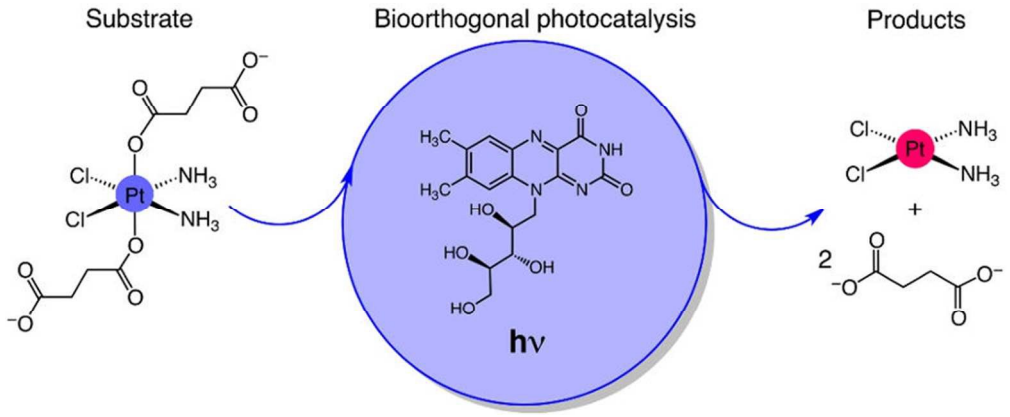

80x32mm (300 x 300 DPI)